Methods and Apparatus for Comprehensive Characterization of Performance Attributes and Limits of Ultrafast Laser Optics

K. R. P. Kafka, T. Z. Kosc, and S. G. Demos

Laboratory for Laser Energetics, University of Rochester

The output power of ultrashort-pulse laser systems can be affected by the ability of the constituent optical components to withstand the generated laser intensity, typically defined by the laser-induced–damage threshold (LIDT). However, large-aperture optics employed in the most powerful laser systems can operate using optics that have sustained some damage with limited performance degradation. In this regime, the operational lifetime of an optic then begins to be governed by the rate of damage growth (increase in size of the damaged area) under subsequent exposure to system laser pulses. Furthermore, recent reports have shown that the optical properties of materials exposed to ultrashort laser pulses can be transiently modified by the high electric-field intensities that can still be below the LIDT fluences. This in turn may cause the modification of the functionality of a device without the initiation of damage.[1] The vast majority of literature to date has focused primarily on measuring the LIDT under single- and multipulse excitation. There is clearly a need to expand the characterization protocols for such optics to include evaluation for the laser-induced–damage growth and functional failure thresholds. The present work describes a system that was developed to provide comprehensive performance characterization, including damage initiation, damage growth, and laser-induced functional degradation for near-infrared, femtosecond-pulsed applications.

A schematic of the testing apparatus developed as part of this work is shown in Fig. 1, with the main components consisting of an ultrafast laser and the experimental damage-testing platform located inside a vacuum chamber. It employs a custom-built optical parametric chirped-pulse–amplification laser system ("Ultraflux," EKSPLA) with 20-fs pulse duration, 820-nm to 970-nm tunable central wavelength, 5-Hz repetition rate, and up to 2-mJ output pulse energy. An *in-situ* dark-field microscope monitors the sample surface to detect damage initiation and/or growth. The reflected beam from the surface of the sample is imaged onto a camera located outside the chamber (L and M7, respectively, in Fig. 1) for laser-induced functional threshold (LIFT) characterization.

Since accurate measurements of damage-growth parameters require the test beam to be significantly larger than the initial and subsequently growing damage site, this system is designed to provide beam area variation of more than one order of magnitude. This was achieved by mounting the beam-focusing optic [off-axis parabolic mirror (OAP) in Fig. 1] on a translation stage together with folding mirror M4 to control the distance from the sample. As these two optics move in tandem, the beam size on the sample changes without disturbing the beam alignment. To facilitate utilization of near-LIDT fluences across a wide range of beam sizes, many of the necessary system features required considerations for management of B-integral (nonlinear phase) that is introduced at high energies in the large-beam configuration. These considerations impacted the design of pulse energy control, polarization control, vacuum window, and beam sampling for diagnostics after all resulting in a calculated total of about $B \approx 1$ at maximum pulse energy.

The operation of the system is demonstrated by the testing of a low-group-delay-dispersion metal-dielectric mirror coating that is designed for broadband enhanced reflection in the near-infrared. This sample was tested at 890-nm central wavelength using 22-fs pulses at a 45°angle of incidence under vacuum environment. The damage-growth measurements were carried out by first initiating damage sites using the smallest beam with a single pulse at a fluence 10% to 15% above the LIDT. This formed a damage site with a diameter of approximately 20 to 30 μm, a precursor from which to measure damage growth. Then the beam size was increased to a 350-μm Gaussian diameter, and each precursor was irradiated by 50 pulses at a fixed fluence. Figure 2(a)

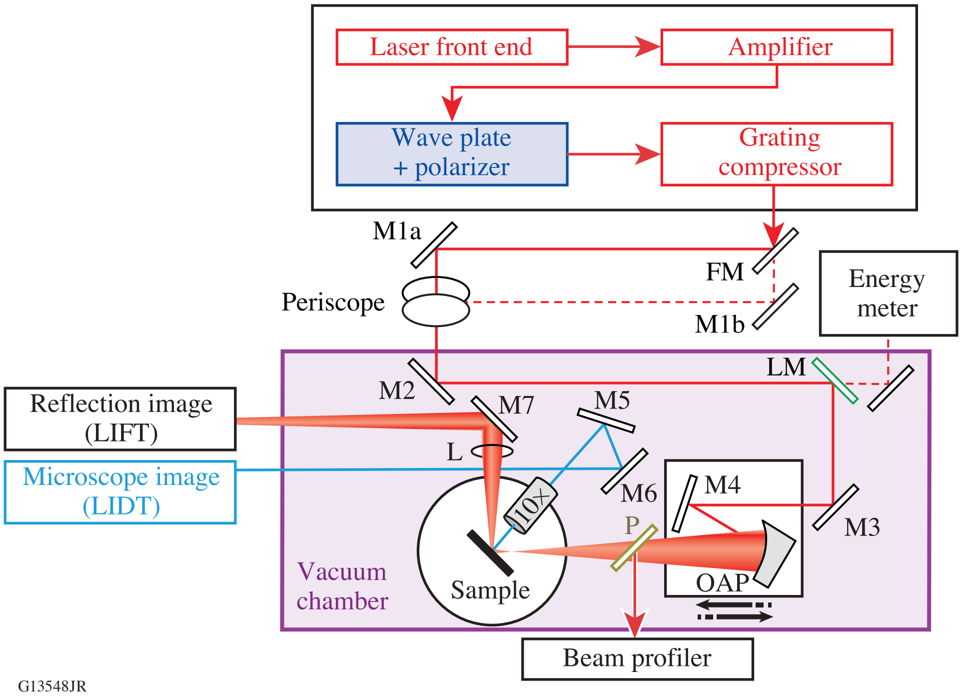

Figure 1
Schematic of performance characterization apparatus. FM: flip mirror; M#: mirror; LM: leaky mirror; OAP: off-axis parabolic mirror; P: pickoff; 10×: 10× microscope objective lens; L: lens.

depicts the size of the single-pulse damage initiation site with respect to the enlarged test beam. The remainder of Fig. 2 shows examples of non-growing and growing sites with each test polarization, imaged off-line using differential interference contrast microscopy. By comparing images of the sample before and after multipulse irradiation, the presence or absence of damage growth was determined for each site, making it possible to calculate the fluence thresholds.

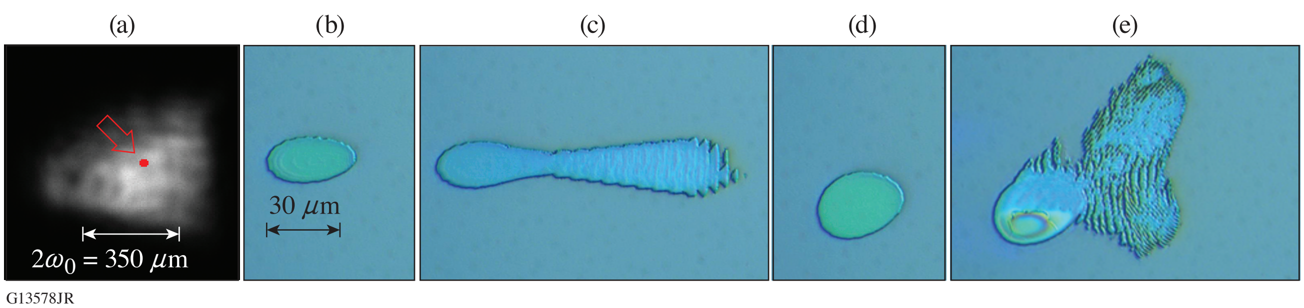

Figure 2
Example morphologies of a damage-growth experiment in optical microscopy. (a) The 30-μm damage initiation site (purposely generated to become the "seed" site for damage-growth experiments) is shown in red overlaid on an example beam profile. For *s* polarization: (b) non-growing site, (c) growing site at 0.34 J/cm^2. For *p* polarization: (d) non-growing site, and (e) growing site at 0.43 J/cm^2. The laser is incident from the left.

The functional performance (a change of the reflection) can be observed by calculating the ratio of reflected beam images from different pulses after first normalizing those images to the total energy. Specifically, reflected beam images represent the ratio between (1) a given test pulse and (2) a previous pulse that did not initiate damage. An example sequence of ratio images showing a detected functional change is depicted in Fig. 3, alongside the concurrent images from *in-situ* dark-field microscopy that show damage has formed. The lineouts across the respective interaction regions are shown in Fig. 3(f). Starting with the pulse in Fig. 3(a), no damage is initiated, and the lineout shows a constant value. In Fig. 3(b), there is clearly a measurable drop of reflectance in the center of the laser beam (indicating functional modification), consistent with energy loss and the onset of damage. The dark-field images shown before and after damage initiation [Figs. 3(d) and 3(e), respectively]. Because in this example the LIFT occurred concurrently to the initiation of damage, the ratio image from the next pulse [Fig. 3(c)] has severely reduced central reflectance (from 1.0 to 0.3) due to low reflectivity of the ablation site. This suggests that a system designed to measure LIFT could simultaneously be a sensitive *in-situ* diagnostic for LIDT measurement with *S*-on-1 or *R*-on-1 protocols.

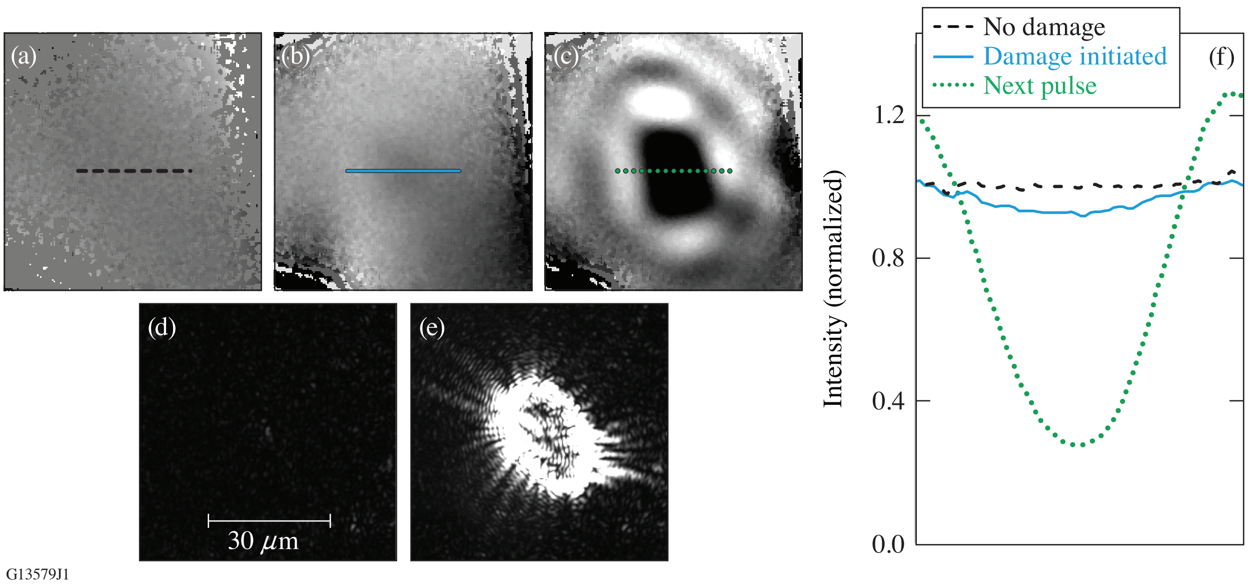

Figure 3
In-situ microscopy of damage formation using [(a)–(c),(f)] functional performance characterization and [(d),(e)] dark-field microscopy. Reflected beam images of (a) a pulse that did not damage, (b) the pulse that initiated damage, (c) the next pulse after damage initiation. Each image in (a)–(c) was normalized by a reflected beam image of a previous pulse that did not initiate damage. (f) The lineouts of the respective reflection images. Dark-field microscope image of the sample, collected (d) before damage initiation, (e) after damage initiation but before the next pulse.

The system and methodology for the characterization of optical components for large-aperture, ultrashort pulse laser systems aims to address current and future needs to support the development of next-generation 100-PW-class laser systems. Achieving the technical objectives required novel implementation of the testing system to avoid problematic nonlinear beam-propagation effects. Initial results underscore that precise damage-testing measurements of optical elements using ultrashort pulses with an expanded and multifaceted definition of damage is important to provide a wide range of information regarding the processes involved that can aid development of improved optic designs and reliable operational fluence limits.

This material is based upon work supported by the Department of Energy National Nuclear Security Administration under Award Number DE-NA0003856, the University of Rochester, and the New York State Energy Research and Development Authority.

1. O. Razskazovskaya *et al.*, Proc. SPIE **9237**, 92370L (2014).